



Aerosol complexity in megacities: From size-resolved chemical composition to optical properties of the Beijing atmospheric particles

Jean-Claude Roger, Benjamin Guinot, Hélène Cachier, Marc Mallet, Oleg Dubovik, Tong Yu

► To cite this version:

Jean-Claude Roger, Benjamin Guinot, Hélène Cachier, Marc Mallet, Oleg Dubovik, et al.. Aerosol complexity in megacities: From size-resolved chemical composition to optical properties of the Beijing atmospheric particles. *Geophysical Research Letters*, 2009, 36, pp.L18806. 10.1029/2009GL039238 . hal-00562372

HAL Id: hal-00562372

<https://hal.science/hal-00562372>

Submitted on 6 May 2021

HAL is a multi-disciplinary open access archive for the deposit and dissemination of scientific research documents, whether they are published or not. The documents may come from teaching and research institutions in France or abroad, or from public or private research centers.

L'archive ouverte pluridisciplinaire **HAL**, est destinée au dépôt et à la diffusion de documents scientifiques de niveau recherche, publiés ou non, émanant des établissements d'enseignement et de recherche français ou étrangers, des laboratoires publics ou privés.



Distributed under a Creative Commons Attribution - NonCommercial 4.0 International License

1 of 5

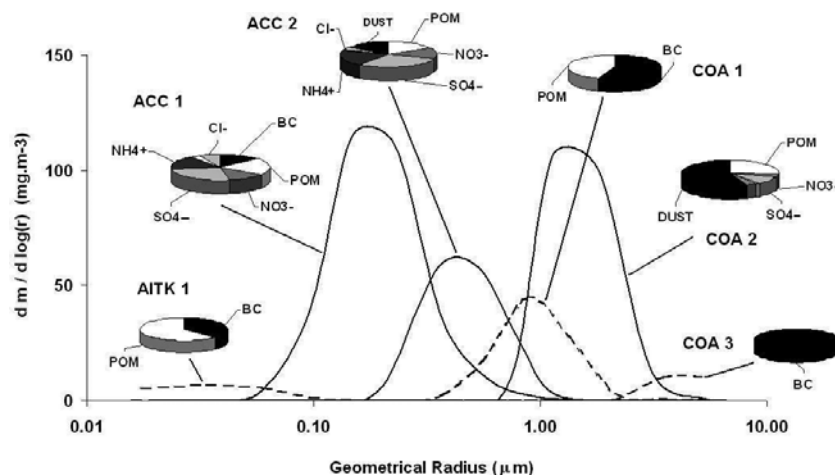


Figure 1. General scheme of the aerosol size-distribution observed for Beijing aerosols (particles sampled with Dekati 13-stage cascade impactors in the range 0.03–10 μm).

each mode being fully defined by its lognormal parameters and its chemical composition. Using adequate algorithms [Roger *et al.*, 2006], these parameters allow retrieval of other properties (aerosol number and optical properties) some of them being compared to direct measurements, thus insuring quality and consistency of data.

2. Mass and Number Size-Distribution of Aerosol and Main Chemical Components

[5] A new process has been developed and applied to aerosol mass and chemical composition in order to sort out all the various aerosol modes and their chemical composition. Based on the size-resolved impactor datasets, and without any pre-defined assessment of mode number, chemical mass distributions consistently end up with 6 modes: one mode in the Aitken size-range (0–100 nm in diameter), two modes in the accumulation size-range (0.1–1.0 μm), and three coarse modes (>1.0 μm). The complex aerosol source pattern in Beijing supports the existence of additional modes compared to models elaborated for urban aerosols of developed countries [Seinfeld and Pandis, 1998; Mallet *et al.*, 2003; Van Dingenen *et al.*, 2004, and references therein], and thus reinforces the need of a new approach to account for aerosol complexity in megacities located in developing megacities. Data consistency firstly allows us to assume that two different types of primary particles, either BC or dust, are present in each mode. We suggest that they may serve as cores for condensation or coagulation processes. Then, the next step is to infer the complete chemical composition of each mode. To that end, in each impactor data set, the distribution of major molar associations is carefully scrutinized. $(\text{NH}_4)_2\text{SO}_4$ and NH_4NO_3 distribution gives consistent evidence for two fine (accumulation) modes organized around a BC core and a dust core separately. For coarse aerosols, dust particles only are found associated to these inorganic ions. Beside these three modes dominated by ion species, there is a clear evidence for three other modes all of them organized around a BC core. One mode is situated in the Aitken size-range while the two others are found in the coarse mode. From this scheme, using an iterative method and a matrix of relative dependence, it is possible to retrieve the distribution of all major aerosol

chemical components throughout the six modes, including particulate organic matter (POM) and dust, respectively estimated from OC and Ca^{2+} as suggested by Guinot *et al.* [2007a]. It may be seen in Figure 1 that five out of the six modes could be made of heterogeneous particles whereas only one appears mostly homogenous in nature (more than 95% of BC). The mode related to ultra-fine particles is termed Aitk1. Although not fully determined due to the impactor geometry limitations (about 2/3 of POM and 1/4 of BC are defined) this mode is overwhelmingly dominated by carbonaceous species and is expected to originate mainly from traffic primary particles or from the coagulation of nucleation particles. Both accumulation modes show an internal mix of inorganic salts and POM, with a core of either BC (for the smallest mode Acc1) or dust (for the biggest mode Acc2). A possible origin of Acc2 particles might reside in the background of fine loess particles originating from the plateau West of Beijing and from resuspended fine dust. In the coarse fraction, the main mode (Coar2) is also an internal mix with an important dust core (representing more than 50% of the mass). The heterogeneous nature of this mode is probably the result of dust-acidic gas interactions previously mentioned for the Beijing aerosol [Guinot *et al.*, 2007b, and references therein]. The two other coarse mode Coar1 and Coar3 are almost pure carbonaceous particles and have probably to be related to truck emissions or industrial inputs [Cachier, 1998]. They represent a non-negligible portion (25% and 10% respectively) of the aerosol coarse fraction either in winter or in summer.

[6] The mass size distribution is then fitted by a lognormal law and distribution is obtained for dry particles as follows. When atmospheric humidity (RH) is higher than 80%, particle radii of the accumulation modes and of the coarse modes (retrieved from impactor data) have been shown to be RH dependent. However as expected, the smallest particles do not exhibit same RH dependency probably because of the significant evaporation of most of their water content under the vacuum met on the first stages (100–200 mbar). The RH dependency follows the Hanel law that has been therefore used to retrieve the dry aerosol radius. The dry aerosol mass distribution (Table 1) clearly enlightens the dominance of the two Acc1 and Coar2 modes. The mass distribution does not

Table 1. Mean Mass $\langle m \rangle$ ($\mu\text{g}\cdot\text{m}^{-3}$) and Standard Deviation for Each of the Dry Aerosol Modes in Winter (Pek1) and Summer (Pek2)^a

| | | Pek1 | | Pek2 | |
|--------|------|---------------------------|-------------------------|---------------------------|-------------------------|
| | | $\langle m \rangle$ (std) | $\langle m \rangle$ (%) | $\langle m \rangle$ (std) | $\langle m \rangle$ (%) |
| Aitk 1 | BC | 0.37 (0.14) | 0.11/30% | 0.36 (0.10) | 0.10/28% |
| Acc 1 | BC | 5.24 (3.12) | 0.85/16% | 4.84 (1.76) | 0.73/15% |
| Acc 2 | dust | 1.79 (1.18) | 0.40/22% | 2.49 (2.10) | 0.83/33% |
| Coa 1 | BC | 0.79 (0.62) | 0.50/63% | 0.37 (0.27) | 0.28/76% |
| Coa 2 | dust | 2.96 (2.16) | 1.48/50% | 5.75 (2.43) | 4.50/78% |
| Coa 3 | BC | 0.16 (0.11) | 0.15/94% | 0.14 (0.07) | 0.13/93% |

^aThe chemical nature (BC or dust) of the probable core is indicated; $\langle m \rangle$ (%) stands for the core mass and percentage. Total number of samples: 19.

exhibit significant changes between winter and summer, particularly for the combustion derived modes formed around a BC core (Acc1, Coar1 and Coar3). The lognormal mass distribution $d m/d \log(r_v)$ is fully characterized for each mode by the mass, the mean radius and its standard deviation. Surprisingly, the dry aerosol radius does not exhibit any seasonality (Table 2) which might denote the presence of a background of pollution all year long, with likely smoothing effects during the two opposite seasons (photochemical production in summer and thermal condensation in winter).

[7] For a purpose of validation, particle number concentration N ($\text{p}\cdot\text{cm}^{-3}$) was calculated from mass size-distributions following Mallet *et al.* [2003]. Particle number is obtained for each mode, using particle density (accounting for the heterogeneous nature of particles and weighing the proper density of each chemical component) and the lognormal mass-distribution parameters (r_v , standard deviation σ). Estimated N values are shown against direct optical measurements obtained from CNC/DPS and GRIMM optical counters (Figure 2) and comparison appears satisfactory. Mass size-distributions may be transformed into number size-distributions and radius data are shown in Table 2. Comparison of measured and retrieved volumic radii of the different modes satisfactorily highlights a good agreement between the two datasets (in auxiliary material).¹ As a matter of comparison too, the procedure used to sort out the 6 log-normal modes from the impactor concentrations has been applied to the monthly aerosol volume data available in the AERONET database (<http://aeronet.gsfc.nasa.gov/>). Similarly, no pre-requisite parameters were set regarding the number of modes, their size or their amplitude. AERONET data strikingly provide same information as impactor data and repeatedly enlighten 2 accumulations modes, and 3 coarse modes (as expected, the very small Aitk1 mode is not easily extractable from AERONET data). The two accumulation modes likely correspond to the Acc1 and Acc2 modes experimentally defined (Table 2). For coarse particles, the smaller AERONET coarse mode may stand for Coa1 and Coa2 that are of very similar size and the second AERONET coarse mode to Coa3 whereas the fourth one corresponding to particles over $10 \mu\text{m}$ in diameter is not sampled by the impactor. The two accumulation mode radii are comparable to those retrieved from AERONET volume size-distributions (Figure 3a). Mean Acc1 radius (0.14 and 0.15 for Pek1 and Pek2 periods) fairly compares with the 0.15 value found with

Table 2. Dry Particle Radius for Each Mode, Respectively for the Volume (\bar{r}_v) and the Number (\bar{r}_n) Size Distributions During the Two Seasons^a

| | | \bar{r}_v | | \bar{r}_n | | STD | |
|--------|--|-------------|-------|-------------|-------|-------|-------|
| | | Pek 1 | Pek 2 | Pek 1 | Pek 2 | Pek 1 | Pek 2 |
| Aitk 1 | | 0.035 | 0.037 | 0.013 | 0.014 | 1.7 | 1.8 |
| Acc 1 | | 0.15 | 0.15 | 0.065 | 0.075 | 1.7 | 1.6 |
| Acc 2 | | 0.42 | 0.44 | 0.295 | 0.300 | 1.4 | 1.4 |
| Coa 1 | | 0.97 | 0.95 | 0.505 | 0.540 | 1.6 | 1.6 |
| Coa 2 | | 1.15 | 1.02 | 0.60 | 0.660 | 1.6 | 1.5 |
| Coa 3 | | 4.56 | 3.87 | 3.330 | 2.730 | 1.4 | 1.4 |

^aStandard deviation unchanged by the mass-to-number conversion.

our sampling-derived procedure. For Acc2 too, AERONET mean radius (0.40 and 0.51) show satisfactory agreement with experimental values (0.40 and 0.42 for Pek1 and Pek2) recalling that sunphotometer data apply to ambient (and not dry) aerosols. Data suggest too that high RH (prevailing in summer) may cause a significant increase of Acc2 particles whereas Acc1 particles appear less prone to water capture.

3. Derived Aerosol Optical Properties

[8] Aerosol radiative effects primarily rely on their single scattering albedo ω_o and their asymmetry parameter g . It has been shown recently that using adequate algorithms, these two parameters could be retrieved based on the chemical composition of each aerosol mode [Roger *et al.*, 2006]. Calculations may account for the heterogeneous nature of particles which are also considered as spheroids [Dubovik *et al.*, 2002]. Evaluated complex refractive indexes show quite similar values during the two experiments for both the real and the imaginary parts which allows assessing a single value over the whole (Pek1 and Pek2) experiment (Table 3). Calculated ω_o and g values at 550 nm and at two different RH for the total aerosol and for each of the 6 identified modes are shown too in Table 3. A comparison with values retrieved from AERONET data was also conducted and the agreement between both data sets appears satisfactory (Figure 3b). As expected, the two accumulation modes (Acc2 and Acc1 particularly) are the most radiatively important modes as

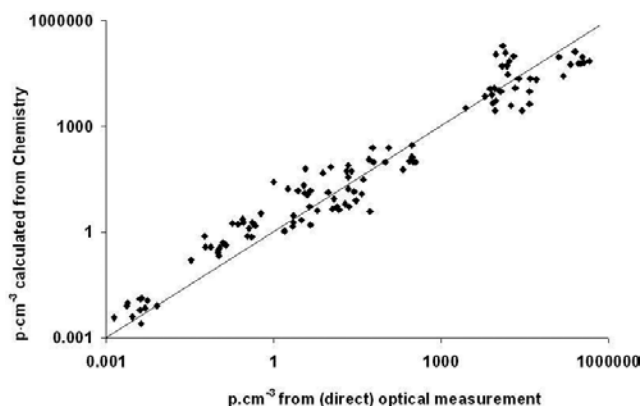


Figure 2. Comparison of direct measurements of particle numbers (CNC/DPS (TSI) and GRIMM optical counters) versus calculated concentration numbers retrieved from mass distributions obtained by impactors ($y = 0.88x + 0.20$; $r^2 = 0.85$).

¹Auxiliary materials are available in the HTML. doi:10.1029/2009GL039238.

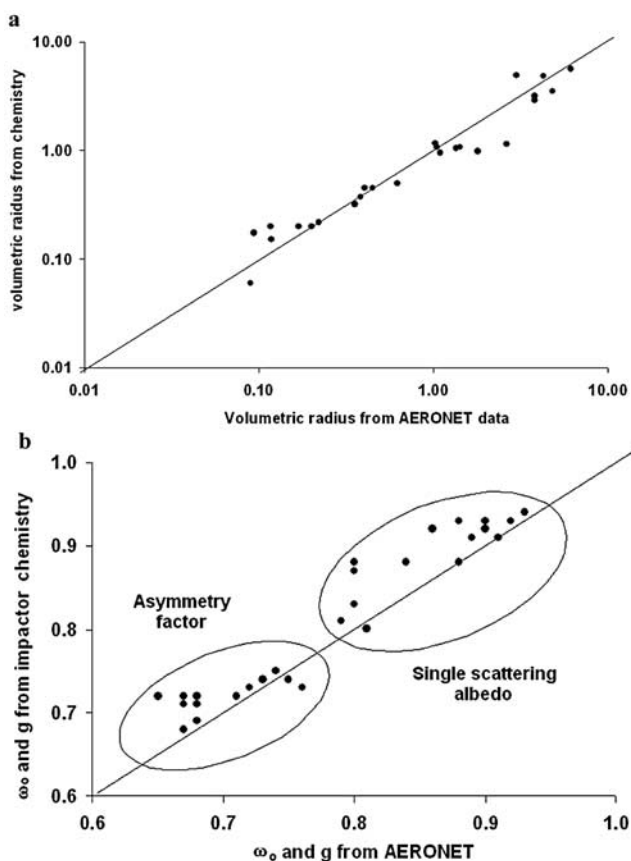


Figure 3. Comparison of AERONET and impactor chemical measurement retrievals. (a) Volumic radius of the different aerosol modes ($y = 0.90x + 0.008$ $r^2 = 0.87$). (b) Single scattering albedos and asymmetry factors of the total aerosol at 550 nm.

they are shown to drive 84% and 80% of the scattering and the absorption, respectively, whereas the role of the two extreme size-modes (Aitk1 and Coar3) is not significant (Table 3). Our optical calculations show that the scattering albedo ω_o of Beijing aerosol is close to 0.90, which is significantly higher than those obtained for other megacities, such as Mexico ($\omega_o \# 0.75$) (Loeffler et al., unpublished material), New Delhi (mean $\omega_o \# 0.68$) [Ganguly et al., 2006] or Kanpur ($\omega_o \# 0.76$) [Tripathi et al., 2005]. Such a high ω_o value, despite the significant BC content in the Beijing aerosol, may be partly explained by the thick coating of scattering species

onto BC particles. BC, the main absorbent species, is thus likely to lose adsorption efficiency and this loss produces an increase of ω_o . Furthermore, significant amounts of fine dust particles are also likely to drive ω_o towards higher values. As for the asymmetry parameter g , the value obtained in our work (0.70) is significantly higher than common values obtained for anthropogenic aerosols. The presence of a significant coarse dust component may explain the importance of scattering in the forward peak. These findings point to the need for an accurate updating of these parameters to be used for the assessment of aerosol optical and radiative properties in Chinese urban areas.

4. Conclusion

[9] Complex situations such as those encountered over Megacities need adapted tools for the accurate modeling of aerosol emissions and transformations. For this purpose a new experimental data processing has been elaborated and validated through various inter-comparisons for the Beijing aerosol and is presented here as a case study. The process produces the distribution of the aerosol particle mass-concentration over several modes which total number is not a-priori assessed. Each mode is defined by its lognormal distribution parameters and its full chemical composition comprising the main components: black carbon (BC), particulate organic matter (POM) and major ions (SO_4^{2-} , NO_3^- , NH_4^+ , Ca^{2+} , Cl^-). The methodology is likely to apply to other megacities at locations where different intense and natural sources, produce high concentrations of particles and precursors, in addition to different atmospheric gas-to-particles processes. The original scheme obtained for Beijing aerosol shows a complexity reflected in the presence of 6 distinct aerosol modes, a situation never encountered in western countries. From the strikingly consistent and repeatable results obtained, it may be inferred that the same sources impact Beijing city whatever the season, with somewhat variability in their relative intensity only. The main straightforward finding relies on the presence of two accumulation modes both bigger ($d \geq 600$ nm) than what is generally inferred for urban aerosols. Furthermore, 5 of the 6 identified modes are found as internal particles organized around a BC core or a dust core. They also point to the intensity of gas-to-particles. Retrieval of aerosol optical properties shows significantly high scattering albedo ω_o (# 0.90) and asymmetry parameter g (# 0.70) values in Beijing, underlining the need for appropriate aerosol studies in complex multi-source situations. The aerosol model may be used for local or regional modeling of aerosol transport and impacts, and

Table 3. Optical Properties of the Beijing Aerosol Modes Calculated at 550 nm^a

| | Refractive Index | | ω_o | | g | | Contribution to the Total Aerosol | |
|--------|------------------|-----------------|------------|------|------|------|-----------------------------------|------|
| | Real | Imaginary | Dry | Wet | Dry | Wet | Scatt. | Abs. |
| Aitk 1 | 1.65 ± 0.04 | 0.17 ± 0.07 | 0.62 | 0.71 | 0.27 | 0.30 | 4% | 4% |
| Acc 1 | 1.60 ± 0.02 | 0.10 ± 0.03 | 0.89 | 0.92 | 0.66 | 0.70 | 60% | 78% |
| Acc 2 | 1.54 ± 0.01 | 0.01 ± 0.01 | 0.98 | 0.99 | 0.75 | 0.76 | 24% | 2% |
| Coa 1 | 1.73 ± 0.04 | 0.36 ± 0.06 | 0.53 | 0.54 | 0.88 | 0.89 | 1% | 14% |
| Coa 2 | 1.55 ± 0.01 | 0.01 ± 0.01 | 0.97 | 0.98 | 0.71 | 0.72 | 10% | 1% |
| Coa 3 | 1.85 ± 0.01 | 0.57 ± 0.01 | 0.59 | 0.59 | 0.89 | 0.90 | 1% | 1% |
| TOTAL | | | 0.86 | 0.91 | 0.69 | 0.73 | | |

^aComplex refractive index of the dry particles (uncertainty stands for standard deviation observed over the whole dataset), single scattering albedo (ω_o) and asymmetry factor (g) for two RH values (dry = 40% and wet = 80%). Contribution of each mode to the total scattering and absorption is also presented.

scientists constructing elaborated air quality models including particle chemistry in megacities may benefit from this work. In particular, due to its sensitivity in the submicron-size fraction, the model may be adequately used to run realistic abatement scenarios for prediction of radiative impacts and may help to develop appropriate pollution controls. The aerosol model may also serve as a first step to evaluate aerosol deposition in the respiratory track and the detailed chemical description of the fine modes might be considered as a useful tool too for research in the field of biological effects of the respirable aerosol [Ramgolam *et al.*, 2009].

[10] **Acknowledgments.** This work was supported by French CNRS (International Department), ADEME, CEA and Ile de France Region. AERONET data was obtained by IAP/CAS (Chen Hongbin).

References

- Baldasano, J. M., E. Valera, and P. Jimenez (2003), Air quality data from 1002 large cities, *Sci. Total Environ.*, **307**, 141–165, doi:10.1016/S0048-9697(02)00537-5.
- Cachier, H. (1998), *UPAC Book on Atmospheric Particles*, pp. 295–348, edited by R. M. Harrison and R. Van Grieken, John Wiley, New York.
- Dubovik, O., B. N. Holben, T. F. Eck, A. Smirnov, Y. J. Kaufman, M. D. King, D. Tanré, and I. Slutsker (2002), Variability of absorption and optical properties of key aerosol types observed in worldwide locations, *J. Atmos. Sci.*, **59**, 590–608, doi:10.1175/1520-0469(2002)059<0590:VOAAOP>2.0.CO;2.
- Ganguly, D., A. Jayaraman, T. A. Rajesh, and H. Gadhavi (2006), Winter-time aerosol properties during foggy and nonfoggy days over urban center Delhi and their implications for shortwave radiative forcing, *J. Geophys. Res.*, **111**, D15217, doi:10.1029/2005JD007029.
- Guinot, B., H. Cachier, and K. Oikonomou (2007a), Geochemical perspectives from a new aerosol chemical mass closure, *Atmos. Chem. Phys.*, **7**, 1657–1670.
- Guinot, B., H. Cachier, J. Sciare, T. Yu, and X. Wang (2007b), Beijing aerosols: Atmospheric interactions and new trends, *J. Geophys. Res.*, **112**, D14314, doi:10.1029/2006JD008195.
- Gurjar, B. R., and J. Lelieveld (2005), New directions: Megacities and global change, *Atmos. Environ.*, **39**, 391–393, doi:10.1016/j.atmosenv.2004.11.002.
- Intergovernmental Panel on Climate Change (2007), *Climate Change 2007: The Physical Science Basis. Contribution of Working Group I to the Fourth Assessment Report of the Intergovernmental Panel on Climate Change*, edited by S. Solomon *et al.*, Cambridge Univ. Press, Cambridge, U. K.
- Mallet, M., J. C. Roger, S. Despiou, O. Dubovik, and J. P. Putaud (2003), Microphysical and optical properties of aerosol particles in urban zone during ESCOMPTE, *Atmos. Res.*, **69**, 73–97, doi:10.1016/j.atmosres.2003.07.001.
- Menon, S., J. Hansen, L. Nazarenko, and Y. Luo (2002), Climate effects of black carbon aerosols in China and India, *Science*, **297**(5590), 2250–2253, doi:10.1126/science.1075159.
- Ramgolam, K., O. Favez, H. Cachier, A. Gaudichet, F. Marano, L. Martinon, and A. Baezza-Squiban (2009), Size-partitioning of an urban aerosol to identify particle determinants involved in the pro-inflammatory response induced in airway epithelial cells, *Part. Fibre Toxicol.*, **6**, 10, doi:10.1186/1743-8977-6-10.
- Roger, J. C., M. Mallet, P. Dubuisson, E. Vermote, H. Cachier, J. P. Putaud, R. Van Dingenen, and S. Despiou (2006), A synergetic approach for estimating the local direct aerosol forcing during the ESCOMPTE campaign, *J. Geophys. Res.*, **111**, D13208, doi:10.1029/2005JD006361.
- Seinfeld, J. H., and S. N. Pandis (1998), *Atmospheric Chemistry and Physics: From Air Pollution to Climate Change*, 1326 pp., John Wiley, New York.
- Tripathi, S. N., S. Dey, V. Tare, and S. K. Satheesh (2005), Aerosol black carbon radiative forcing at an industrial city in northern India, *Geophys. Res. Lett.*, **32**, L08802, doi:10.1029/2005GL022515.
- Van Dingenen, R., *et al.* (2004), A European aerosol phenomenology—1: Physical characteristics of particulate matter at kerbside, urban, rural and background sites in Europe, *Atmos. Environ.*, **38**, 2561–2577, doi:10.1016/j.atmosenv.2004.01.040.
- H. Cachier, Laboratoire des Sciences du Climat et l'Environnement, CEA, CNRS, Bat 12, avenue de la Terrasse, F-91198 Gif-sur-Yvette CEDEX, France.
- O. Dubovik, Laboratoire d'Optique Atmosphérique, CNRS, Bat P5 Cite scientifique, F-59655 Villeneuve d'Ascq CEDEX, France.
- B. Guinot and M. Mallet, Laboratoire d'Aérodologie, OMP, Université Paul Sabatier, CNRS, 14 avenue Edouard Belin, F-31400 Toulouse CEDEX, France.
- J.-C. Roger, Laboratoire de Météorologie Physique, UMR 6016, Université Blaise Pascal, CNRS, 24 avenue des Landais, F-63177 Clermont-Ferrand CEDEX, France. (roger@opgc.univ-bpclermont.fr)
- T. Yu, Beijing Municipal Environmental Monitoring Centre, 14 West Chegongzhuang Road, Beijing 100044, China.